

Gasification operational characteristics of 20-tons-Per-Day rice husk fluidized-bed reactor

Sung Jin Park^a, Seong Hye Son^a, Jin Woo Kook^b, Ho Won Ra^a, Sang Jun Yoon^a,
Tae-Young Mun^a, Ji Hong Moon^a, Sung Min Yoon^a, Jae Ho Kim^a, Yong Ku Kim^a,
Jae Goo Lee^a, Do-Yong Lee^b, Myung Won Seo^{a,*}

^a Clean Fuel Research Laboratory, Korea Institute of Energy Research (KIER), 152 Gajeong-ro, Yuseong-gu, Daejeon, 34129, Republic of Korea

^b Kyungwon Tech (KW Tech), 81 Yatap-ro, Bundang-gu, Seongnam, Gyeonggi-do, 13497, Republic of Korea

ARTICLE INFO

Article history:

Received 8 April 2020

Received in revised form

8 December 2020

Accepted 7 January 2021

Available online 12 January 2021

Keywords:

Gasification

Rice husk

Equivalence ratio

Tar removal

Computational particle fluid dynamics

ABSTRACT

Converting rice husk into energy is a promising method of generating renewable energy and reducing greenhouse gas emissions. The characteristics of rice husk gasification were investigated at an equivalence ratio (ER) of 0.20–0.35 and a gasifier temperature of 700–850 °C in a 20-tons-per-day (TPD) bubbling fluidized-bed gasifier system. The optimal conditions of the gasification operation were an ER of 0.20 and gasifier temperature of 800 °C. The low heating value of the gas product and cold gas efficiency were 1373.18 kcal/Nm³ and 70.75%, respectively. After passing the generated gas through the gas cleaning units, it was confirmed that the tar in the product gas was removed with an efficiency of 98%. The cleaned product gas was used for the operation of 400 kW_e gas engine. Pressure loss often occurred at the bottom of the gasifier during the gasification operation; we found that the agglomerates generated by the gasification process caused it. Computational particle fluid dynamics simulations were performed to investigate the fluidizing characteristics of agglomerates. To prevent the pressure loss caused by the agglomerates, the stable control of temperature inside the gasifier is needed and an ash removal device remove agglomerates should be installed to maintain stable long-term operation.

© 2021 Elsevier Ltd. All rights reserved.

1. Introduction

Industrialization and the high growth rate of the global economy has resulted in an increasing global demand for energy. Although fossil fuels are commonly used as energy sources around the world, such resources are associated with the emission of high amounts of greenhouse gases such as CO₂. To mitigate greenhouse gas emissions in the energy sector, renewable energy sources such as biomass, solar energy, and wind can be used as alternatives to replace fossil fuels. Biomass use, in particular, can be carbon-neutral; biomass gasification is an optimum technology for converting biomass into heat and electricity through engines, turbines, and boilers [1].

Among all the potential biomass sources, rice husk represents an attractive feedstock because it is a major agricultural product with an annual production rate of 148.2 million tons globally [2].

Rice husk is usually disposed of or used in low-value applications such as barn matting. Previous research has indicated that rice husk has the potential to be a high-value material as feedstock for gasifiers to generate heat and electricity [3]; rice husk ash produced through gasification can be used for the production of nano-structured silica, silicon, aerogel, and brick-based products [4].

Conversion processes for biomass include biological, thermochemical, and physical methods. The thermochemical conversion process involves pyrolysis, gasification, and combustion. During gasification, heat and electricity can be generated using low energy density fuels such as biomass and waste. The gas produced through gasification can generate heat and electricity through gas engines, turbines, and boilers; it consists of hydrogen (H₂), carbon monoxide (CO), methane (CH₄), and tar. The gasification process uses gasifying agents such as air, oxygen (O₂), carbon dioxide (CO₂), and steam (H₂O). Operation parameters of biomass gasification include the equivalence ratio (ER), gasifying agent, catalyst, and bed temperature.

The ER is defined as the ratio of O₂ needed for the complete stoichiometric combustion of the fuel; it is further explained in

* Corresponding author.

E-mail address: mwseo82@kier.re.kr (M.W. Seo).

Section 2.3. Siedlecki and de Jong [5] reported that the optimum ER for achieving a high heating value of the gas product is 0.20–0.40. The cold gas efficiency (CGE) of the product gas reaches the maximum at an ER of 0.20–0.30 and decreases at a higher or lower ER [6].

The gasifying agent influences the product gas composition. When steam is used in gasification, the heating value of the product is higher than that when air is used [6] because air gasification generates product gas diluted by N₂ [7]. However, steam gasification has several disadvantages, namely, requiring additional heat to produce steam and low conversion efficiency.

Bed temperature is also an important operation parameter in gasification as it influences both the heating value and product gas composition. The product gas is generated by the main reaction processes, e.g., oxidation, partial oxidation, water–gas (primary and secondary), water–gas shift, the Boudouard, and steam reforming reactions [8]. Increasing the bed temperature improves the carbon conversion efficiency and the product gas yield. The optimum bed temperature is 700–800 °C, leading to a high yield of H₂ and CO in the product gas [9]. However, higher temperatures will induce ash fusion and the production of undesirable gases such as NO_x [10].

Tar, an unwanted gasification product, is a hydrocarbon that comprises single and multiple ring aromatic compounds [11]. As tar results in many problems during biomass gasification, tar removal is important for continuous and stable gasification operation. To reduce the tar content in the product gas, a catalyst such as dolomite or olivine; a cleaning unit, e.g., condensers, electrostatic catchers; and cooling, demisting, and filter (CDF) systems, are widely used.

For rice husk gasification, both fixed-bed (downdraft) and fluidized-bed gasifiers can be used. Fixed-bed gasifiers, however, suffer from hot spots owing to difficulties in heat control and a high amount of tar generation, causing blockages, plugging, corrosion, and finally, serious operational and maintenance problems. Conversely, stable fluidized-bed gasifier operation is possible with uniform temperature control and high heat and mass transfer rates of rice husk and bed material.

In addition, the emissions of NO_x and SO_x are low as the operation temperature of bubbling fluidized-bed reactors is relatively low (700–800 °C). The amount of tar generation in fluidized-bed gasifiers is relatively lower than that of fixed-bed gasifiers. In this study, we focused on the application of a fluidized-bed gasifier for rice husk gasification. Table 1 summarizes previous studies on rice husk and mixtures in pilot-scale fluidized-bed gasifier experiments [9,12–20].

Although much research has been conducted on rice husk gasification characteristics in a fluidized-bed gasifier, only a small number of studies have been conducted on integrated gasifier–gas cleaning–gas engine systems. In this study, the optimal conditions of the rice husk bubbling fluidized-bed gasification system were determined with variances in ER and temperature. The CDF system, which can remove tar from the product gas, was successfully adapted and its feasibility for gas engines was assessed. The pressure loss phenomenon due to the formation of silica agglomerates in the fluidized bed was observed and analyzed by CPFD simulation. A recommendation for the long-term operation of a rice husk bubbling fluidized-bed gasifier is proposed for the scale-up to the demonstration scale.

2. Materials and methods

2.1. Materials

Table 2 shows the results of proximate, ultimate analyses of rice

husk and X-ray fluorescence spectrometry (XRF) analyse of the rice husk ash. Rice husk ash is mainly composed of silica (SiO₂) and other alkali metals such as K₂O and CaO, which can form agglomerates with bed material.

The rice husk and silica sand properties are presented in Table 3.

Rice husk is unfavorable for fluidization because it has low sphericity ($\Phi_s = 0.19$) and density (ρ_b of 111 kg/m³ and ρ_s of 505 kg/m³). According to Geldart's classification system [23], the rice husk belongs to Geldart's Group D and has spoutable characteristics.

Silica sand was used as bed material because it belongs to Geldart's Group B, which comprises materials suitable for fluidization. The silica sand had a particle mean diameter, d_p of 456 μ m, Φ_s of 0.92–0.96, and ρ_s of 2642 kg/m³. Additionally, silica sand has advantages in that it is very inexpensive and can be used to maintain a uniform temperature in a gasifier because of its suitable heat transfer effect.

2.2. Apparatus

Fig. 1 shows a photograph and schematic diagram of the 20-tons-per-day (TPD) rice husk bubbling fluidized-bed gasifier system.

The overall system consists of a duct burner; a forced-draft (FD) fan; a rice husk screw feeder; a bubbling fluidized gasifier (1.6 m I.D. \times 11 m height); a cyclone; a first condenser; a second condenser; a U-shape scrubber; a cooling, demisting, and filter (CDF) system; an induced draft (ID) fan; a buffer tank; and a gas engine with a 400-kW_e power-generation capacity. The FD fan was used to inject air into the bubbling fluidized-bed gasifier for air gasification and fluidization of the silica sand. The feeder type was a screw feeder, which supplied a constant source of rice husk. The bubble cap type distributor for the fluidized silica sand and rice husk was installed at the bottom of the gasifier. A duct burner fueled by diesel was used to pre-heat the gasifier to 500 °C. K-type thermocouples and pressure transducers were installed in the axial direction to measure the temperature and monitor pressure for the fluidization state inside the reactor.

The cyclone removed the solid particles in the product gas. The condensers and U-shape scrubber were used to remove tar in the product gas. As the tar should be removed ahead of gas engine applications, a CDF system was used to clean the product gas. Afterward, the product was passed through a non-dispersive infrared (NDIR) sensor-type gas analyzer (AO2000 Series, ABB) to analyze the product gas composition. The gas engine was capable of generating 400 kW_e; Table 4 shows the technical parameters of the gas engine.

2.3. Experimental method

Table 5 shows the operating conditions for the rice husk bubbling fluidized-bed gasifier system.

The ER can be calculated using the following equation [24]:

$$ER = \frac{\text{External } O_2(\text{air}) \text{ supply/fuel input}}{\text{Stoichiometric } O_2(\text{air}) \text{ requirement/fuel input}} \quad (1)$$

where ER = 0 refers to pyrolysis, ER > 1 to combustion, and 0 < ER < 1 to gasification. Usually, the ER ranges from 0.15 to 0.40 for biomass gasification. Increasing the ER will result in low yields of H₂ and CO and high yields of CO₂.

The duct burner was fueled by diesel and used to increase the temperature of silica sand inside the gasifier to 500 °C in the pre-heating stage. Air as the gasifying agent was introduced into the gasifier. When the silica sand temperature reached 500 °C, rice husk was injected into the gasifier at a rate of 111 kg/h. This

Table 1
Summary of previous studies on rice husk and mixtures in a pilot-scale fluidized-bed gasifier.

Author	Reactor/fuel	Feeding rate (kg/h)	Reactor diameter/height (m)	Temperature (°C)/pressure (bar)	Equivalence ratio (-)	Gasifying agent	Tar (g/Nm ³)	Thermal power output (kW _e)	Remarks
Makwana et al. [9]	Bubbling fluidized-bed/rice husk	25–31.35	0.21/1.6	750–850/ambient	0.30, 0.33, 0.35, 0.38	Air	2.73	–	Electricity consumption was low and there were no clinkers. Increases in the ER reduced the tar content in the product gas. Removed tar using dolomite as a catalyst.
Subramanian et al. [12]	Fluidized-bed/rice husk, coir pith, sawdust	40	0.32, 0.2/2.5	800–900/ambient	0.30–0.50	Air	–	–	Three agricultural wastes were used as gasification fuel and comparisons were made of the product gas. With increases in the ER, the content of CO ₂ increased and the content of CO decreased.
Karmakar et al. [13]	Bubbling fluidized-bed/rice husk	50	0.5/1	600–800/ambient	0.25, 0.35, 0.45	Air	–	–	Increases in the temperature increased H ₂ and CO. Increases in the ER increased the higher heating value (HHV) and CGE, as well as carbon conversion.
Behainne and Martinez [14]	Bubbling fluidized-bed/rice husk	50	0.3/3	700–900/ambient	0.20–0.40	Air	–	73.82	At a height of material above 0.3 m, the carbon conversion increased because the mass and energy transfer conditions increased. Conditions were suitable for the design of a small-scale power generation system using rice husk as fuel.
Mansaray et al. [15]	Fluidized-bed/rice husk	61.2	0.255/2.7	665–830/ambient	0.25, 0.30, 0.35	Air	–	–	The differential pressure decreased when the air velocity increased. The production of product gas was not significantly affected by the fluidization velocity. However, it increased as the ER increased.
Zhou et al. [16]	Circulating fluidized-bed/rice husk, sawdust	–	0.2, 0.8/2.2	650–900/ambient	0.22–0.34	Air	–	–	The ER was shown to be an important operating condition for determining the heating value of the product gas. The gasification efficiency of rice husk reached 77% at ER = 0.28.
Ramírez et al. [17]	Bubbling fluidized-bed/rice husk	–	0.3/3	812/ambient	0.32	Air	–	70	With an ER = 0.32, the average product gas composition was H ₂ , 4.56%; CO, 11.1%; and CH ₄ 3.45%. The cold gas efficiency was 38.79%.
Yin et al. [18]	Circulating fluidized-bed/rice husk	1500	1.25/7.4	700–850/ambient	0.2–0.25	Air	<0.1	1000	The composition of the product gas during continuous operation was affected by the moisture content of the rice husk.
	Bubbling fluidized-bed/rice husk	400–1500	1.4, 2.0/8.5	700–800/ambient	0.12–0.30	Air	<0.1	700–4000	Increasing the temperature decreased the gas heating value. The water content of the fuel had an influence on the operation of the gasification system.
Wu et al. [19,20]	Circulating fluidized-bed/rice husk, cotton stalk	3000–6000	3/20	700–810/ambient	Unknown	Air	–	1000	The gasification system was run continuously and safely for four years. The tar should be removed through the development of refineries for continuous operation. A total of 8000 h of experimental operation was conducted stably and the overall system efficiency improved. For safe continuous operation, tar was removed using a cleaning equipment.

increased the bed temperature to 800 °C because of the combustion of rice husk. When the fluidized-bed gasifier temperature reached 800 °C, the duct burner was turned off and the rice husk and air-injection feed rate was controlled to meet the desired gasification conditions.

3. Results and discussion

This section consists of four subsections. The gasification operation characteristics with the variation of ER were determined in the first section. The second section describes the tar content and removal efficiency of each gas cleaning unit at steady-state conditions. At the optimal operating condition, the gasification characteristics such as temperature, flow rate, and gas composition of product gas were presented in the steady-state operation characteristics section. The abnormal pressure loss phenomenon detected during the operation is analyzed in the final section with a recommendation for the successful long-term operation of a gasifier system.

3.1. Effect of ER

The reactions of gasification in the bubbling fluidized-bed reactor are as follows [25].

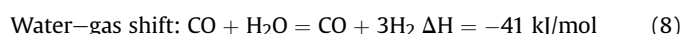
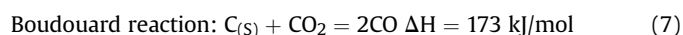
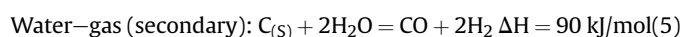
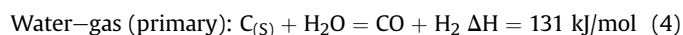
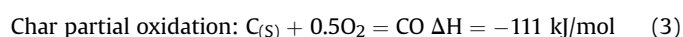
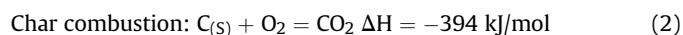


Table 2
Proximate, ultimate analyses of rice husk and XRF analyse of rice husk ash.

Characteristics	Value															
Proximate analysis (As received)																
Moisture (%)	12.35															
Volatile matter (%)	59.33															
Ash (%)	11.36															
Fixed carbon (%)	16.96															
Ultimate analysis (Dry ash free basis)																
C (%)	49.64															
H (%)	6.30															
O (%)	42.20															
N (%)	1.81															
S (%)	0.05															
LHV (kcal/kg)	3690															
XRF	SiO ₂	K ₂ O	CaO	P ₂ O ₅	MgO	MnO	SO ₃	Cl	Fe ₂ O ₃	Al ₂ O ₃	Cr ₂ O ₃	SnO ₂	ZnO	CuO	Na ₂ O	NiO
Rice husk ash	90.37	6.30	1.21	1.02	0.35	0.28	0.15	0.10	0.09	0.07	0.05	0.04	0.02	0.01	0.01	0.01

Methane reforming: $\text{CH}_4 + \text{H}_2\text{O} = \text{CO} + 3\text{H}_2$ $\Delta H = 206 \text{ kJ/mol}$ (9)

The ER is an important parameter in air gasification. Increasing or decreasing the ER influences the product gas composition, lower heating value (LHV) of product gas, and CGE. Fig. 2 shows the measurement results of the product gas composition, LHV of the product gas, and CGE.

When the ER was increased, the product gas composition of H_2 , CO, and CH_4 decreased from 4.38 to 1.11%, 22.12 to 10.34%, and 6.91 to 2.48%, respectively. Conversely, the concentration of CO_2 increased from 15.86 to 17.75% as the ER increased. Mansaray et al. [15] conducted a study on the gasification characteristics of rice husk according to the increase in ER. At ER ranges of 0.18–0.32, the gas composition of H_2 , CO, CH_4 , and CO_2 ranged from 3.25 to 4%, 12.29–19.9%, 1.84–2.9%, and 14.45–17.42%, respectively, similar to this study.

The yield of CO_2 increased with the increased oxidation of carbon in the rice husk as seen in Eq. (2); this is because the oxygen injection amount increased with increasing ER. Several studies have investigated the effects of ER and reported that the amounts of H_2 and CO decrease and the composition of CO_2 increases with increases in the ER [9,13,15,26].

The LHV of product gas decreased from 1373.18 to 555.05 kcal/ Nm^3 as the ER was increased because the concentrations of CH_4 and other light hydrocarbons, which have large heating values, were reduced. Additionally, the product gas was diluted by the increasing N_2 [16].

The gasification performance was evaluated by the CGE. The CGE decreased from 70.75 to 44.23% because the increasing ER generated more CO_2 in the product gas. Panaka and Trisaksono [27] also reported that general values of the CGE of a biomass gasifier are typically between 45% and 67%.

3.2. Tar removal efficiency

During gasification, the formation of tar can cause problems such as corrosion, fouling, and blocked pipes in equipment such as gas engines and turbines. These problems subsequently will result in an increase in operational costs. To achieve continuous operations, the removal of tar from the product gas is an important issue. The primary method, which involves heating to high temperatures or using catalysts, can reduce the tar content from high-weight hydrocarbons to low-weight hydrocarbon. The secondary method involves the use of a gas cleaning unit such as a condenser or scrubber to remove tar. Table 6 shows the tar contents when the optimal operation conditions of gasification resulted in an ER of 0.20. These contents were measured using a tar sampling device

after the tar passed through the cyclone, condenser, scrubber, and CDF system.

The tar sampling device is the same as that described in our previous work [28]. The CDF system reduces the temperature of the product gas below the dew point through water cooling. The tar is changed into a micro water-mist and then removed by the coalescing filter. The tar content after the cyclone was as high as 2.24 g/ Nm^3 because the cyclone only removed the dust in the product gas. The tar removal efficiency was 86.1% after passing through the first and second condensers and increased to 89.3% after passing through the U-shape scrubber. The tar removal efficiency was 98% after passing through the CDF system, which represents a high removal efficiency; the tar content was 0.046 g/ Nm^3 . Makwana et al. [9] conducted a study on tar reduction using dolomite as a catalyst. The tar content in the product gas is 2.73 g/ Nm^3 , whereas the tar removal rate was found to be 41–46%. Yin et al. [18] used gas cleaning units to reduce tar in the product gas and the tar content in the product gas was less than 0.1 g/ Nm^3 , which is adequate for long gas-engine operation. The product gas from the bubbling fluidized-bed gasification system can be used in gas engines according to the recommendations of Hasler and Nussbaumer [29], who reported that the tar tolerance for gas engine operations is below 0.1 g/ Nm^3 . As a result, the product gas can be stably supplied for gas engine to generate electricity at a capacity of 400 kW_e.

3.3. Steady-state operation characteristics

The composition and LHV of the product gas and CGE of the gasifier were analyzed throughout changes in the ER as shown in Section 3.1. The optimal condition of the ER was found to be 0.20 in terms of the LHV of product gas and CGE of the gasifier. Fig. 3 shows the temperature, pressure, and gas composition during steady-state operation at an ER of 0.20.

Operating conditions at an ER of 0.20 included a feedstock injection rate of 669 kg/h and an air flow rate of 479 Nm^3/h (real-time basis). The gasifier temperature was maintained between 700 and 800 °C and continuous operations were conducted over 14 h.

The temperature of the air box is marked as T1; it decreased because the duct burner was turned off. T2 and T3 represent the temperature and P-1 (0.35 m from distributor) and P-2 (1.35 m from distributor) indicates the pressure of the lower part of the gasifier.

The average temperature of the gasifier was around 800 °C and P-1 was maintained at around 1300 mmAq. The higher part of the gasifier was maintained at a negative pressure to inject the rice husk smoothly into the gasifier. The temperature of the product gas decreased to 55 °C (T12) after the first and second condensers. The

Table 3
Main characteristics of the rice husk and silica sand.

Specification		Silica sand	Rice husk
Particle mean diameter (d_p)	(mm)	0.456	Length: 7–8 Width: 2–3 Thickness: 0.2
Particle density (ρ_s)	(kg/m ³)	2642	505
Apparent density (ρ_b)	(kg/m ³)	1188	111
Sphericity (Φ_s)	(–)	0.92–0.96 (Theoretical calculation)	0.19 (Theoretical calculation)
Minimum fluidizing velocity (U_{mf})	(m/s)	0.18 (R.T.) 0.08 (800 °C) (Theoretical calculation [21])	0.46–0.6 (Literature [22])
Geldart's classification [23]		B	D

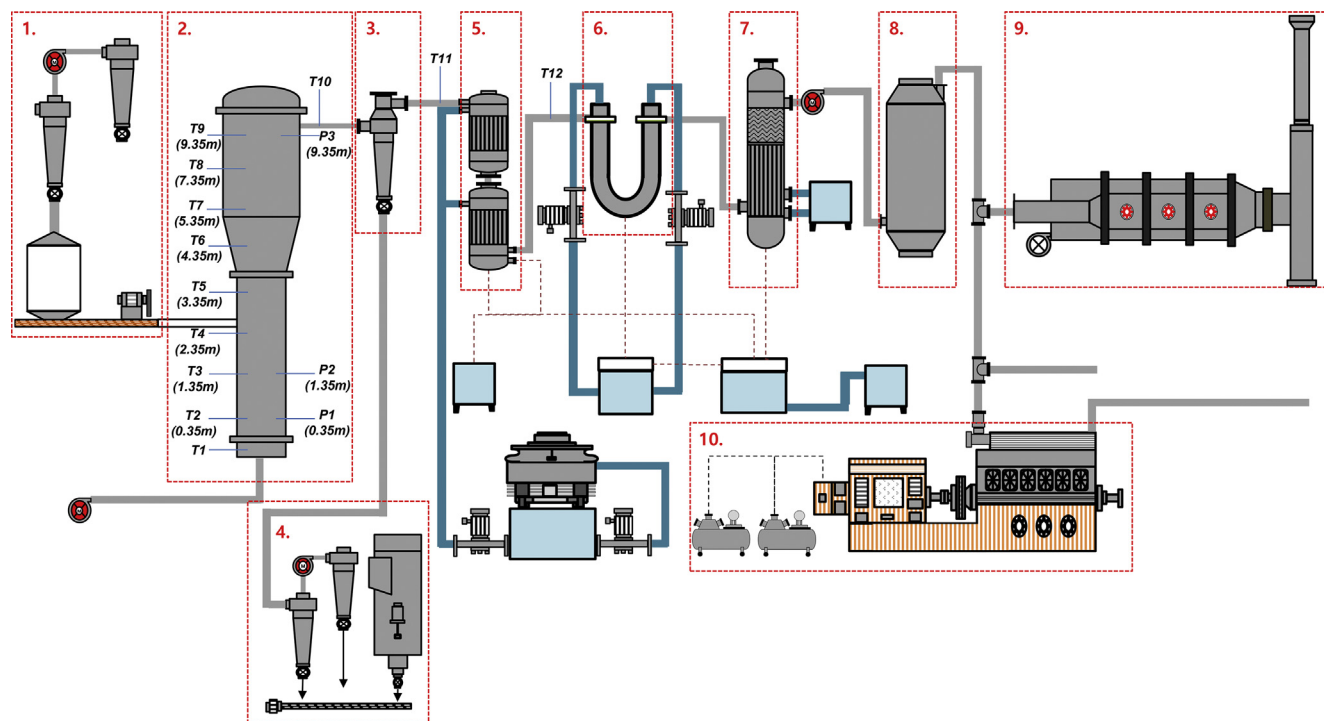


Fig. 1. Schematic diagram of the 20 TPD rice husk bubbling fluidized-bed gasifier system (1: Feeder system, 2: Bubbling fluidized-bed gasifier, 3: Cyclone, 4: Fly ash removal system, 5: First and second condensors, 6: U-shape scrubber, 7: CDF system, 8: Buffer tank, 9: Combustion furnace and flare stack, and 10: Gas engine).

Table 4
Parameters of the 400 kW_e gas engine.

	Contents	Parameters
Type	—	Four stroke pressure engine
Quantity	—	1
Design standards	Rated power of the engine	440 kW _e
	Rated power of the generator	400 kW _e
Specifications	Gas consumption	1070–1510 Nm ³ /h
	Supply engine gas pressure	2 kPa
	Explosion pressure	<5.5 MPa

Table 5
Operating conditions of rice husk bubbling fluidized-bed gasification.

Operating condition	Operational range
Air flow rate (Nm ³ /h)	253–837
Feeding rate (kg/h)	354–669
Temperature (°C)	700–850
Equivalence ratio (ER)	0.20–0.35

average contents of the product gas at an ER of 0.20 were as follows: H₂, 4.38%; CO, 22.12%; CH₄, 6.91%; and CO₂, 15.86%. The average LHV of the product gas and CGE were 1373.18 kcal/Nm³ and 70.75%, respectively.

The product gas that was produced from the gasifier was used to operate a gas engine in this study. When the four-stroke gas engine was operated, the operations conditions were 514 rpm and 400 mmAq for the injection pressure of the product gas. The average flow rate of the product gas was 1090 Nm³/h. This flow rate was maintained during engine operation. To generate electricity, the operation load was constant at 400 kW_e. Overall, the net electricity efficiency was calculated as 14% for the power generation of 400 kW_e. The typical range of net electricity efficiency of the biomass fluidized-bed air gasification is 10–30% [25].

3.4. Pressure loss phenomenon during operations

Fig. 4 shows the temperature, pressure, flow rate, and gas composition when the pressure loss phenomenon at the bottom of the gasifier (P-1, P-2) occurred during abnormal gasification operations.

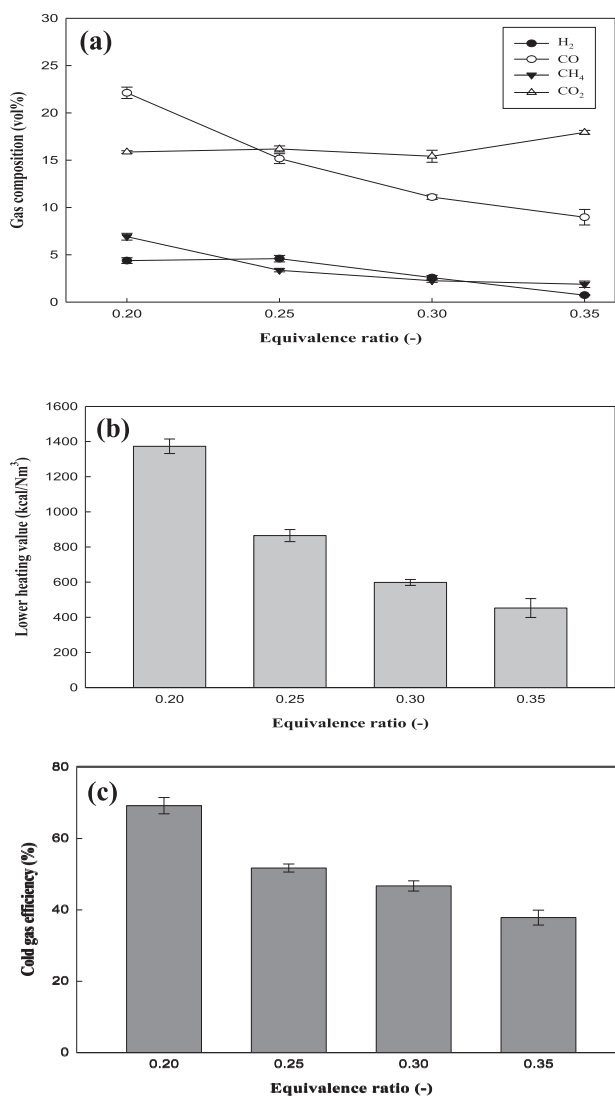


Fig. 2. Effect of the equivalence ratio on (a) the gas composition, (b) lower heating value of gas, and (c) cold gas efficiency.

Fig. 5 shows the schematic diagram of the change of temperature in the gasifier and product gas according to the pressure loss.

First, pressure loss was caused by agglomerate formation at the bottom of the gasifier (P-1, P-2), then, the temperature at the upper part of the gasifier (T3-T9) suddenly increased up to 1000 °C as more air/oxygen was introduced to the feeder side of the gasifier. After the increasing temperatures at the top of the gasifier, the H₂, CO, and CH₄ contents of the product gas decreased and the CO₂ content increased. Additionally, defluidization seemed to occur at the bottom of the gasifier as the temperature (T2) decreased to 700 °C. The reason for the increased CO₂ content of the product gas was due to the shift from gasification to combustion because of the

channeling and defluidization phenomenon between the silica sand particle and agglomerates.

Table 7 shows the slagging and fouling index predicted using the XRF results of the rice husk [30].

The overall decision on the slagging and fouling index would be moderate (5 Slight, 2 Severe). For rice husk, the silica–alkali ratio influenced the formation of aggregates.

Agglomerates were produced after gasification and XRF analyses were performed. Table 8 and Fig. 6 show the XRF analysis results for the agglomerates.

The agglomerates shown in Fig. 6A and B contained high contents of MgO and Fe₂O₃ and were mixed with refractories broken from the reactor during gasification due to impacts with the wall. The agglomerate displayed in Fig. 6C was the main type of agglomerates, with high SiO₂ content; rice husk ash was melted during gasification and aggregates with a crystal structure were formed.

The fluidizing characteristics inside the bubbling fluidized bed was modeled using a commercial CPFD Barracuda® software. In Barracuda, the fluid phase, particle momentum, and fluidizing characteristics are calculated using Multiphase particle-in-cell (MP-PIC) numerical methods [31,32]. The equations of continuum phase and particulate phase can be found elsewhere [33]. The grid design of the bubble fluidized-bed gasifier was constructed to simulate the equipment used in this study and the total number of cells in the model was 26030. The air velocity was 0.72 m/s (4 U_{mf}).

In the CPFD simulations, it was assumed that particles do not move by agglomerates near the distributor. The gasifier temperature was set to 1073.15 K and the pressure change around the gasifier distributor was analyzed. The gasification reaction was not considered in this study. Table 9 shows the parameters used in the CPFD simulations.

The total number of particles was 1.79×10^{10} . Particles were stacked at the bottom of the gasifier to simulate agglomerates accumulated near the distributor. Fig. 7 shows the results of the CPFD simulations.

The simulation results showed that the flow was smoothly generated on the sides where the agglomerates had not accumulated. The average axial pressure profile shows general decreasing trend of pressure with increasing height in the bubbling fluidized bed reactor meaning that the pressure loss was not detected in CPFD simulation. However, the stacked agglomerates marked as yellow circle in Fig. 7 formed a dead zone near the distributor. As agglomerates cause channeling, defluidization, and hot spots in the reactor, they should be removed during gasification by a bed ash-discharge system.

To prevent the pressure loss caused by agglomerates, an agglomerate removal device that can remove agglomerates generated during gasification should be installed to maintain the optimum operating conditions for rice husk gasification. Previous studies have shown that an agglomerate removal device can be installed at the bottom of the gasifier to remove agglomerates during gasification but high portions of silica sand bed materials can be lost [36,37]; therefore, the recirculation of silica sand is required. Another method to reduce agglomerates is to add additives such as kaolin and dolomite into the gasifier to inhibit

Table 6

Tar content and removal efficiency at each sampling position.

Sampling position	Tar content (g/Nm ³)	Tar removal efficiency (%)
After cyclone	2.2409	—
After condenser	0.3125	86.1
After scrubber	0.2406	89.3
After cooling, demisting, and filter (CDF) system	0.0455	98

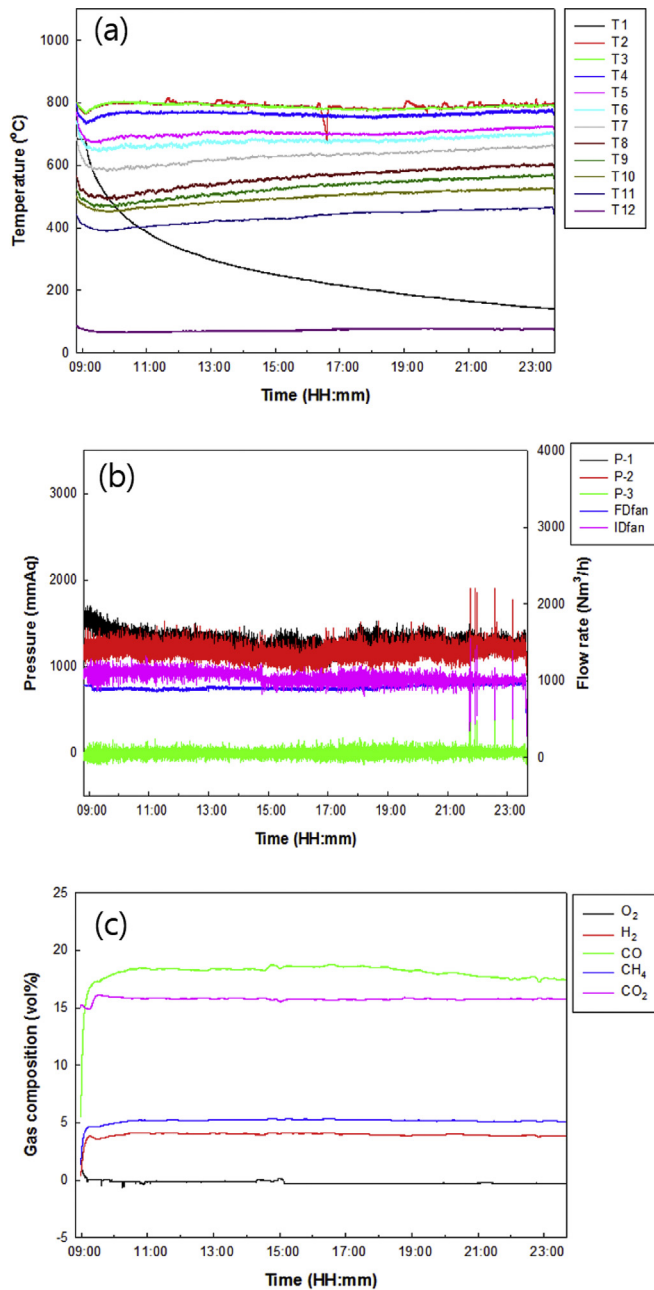


Fig. 3. (a) Temperature, (b) pressure and flow rate, and (c) gas composition during steady-state operation (ER = 0.20).

agglomeration tendency [38].

4. Conclusion

A 20-TPD rice husk bubbling fluidized-bed gasifier was developed and investigated. To determine the optimum conditions for rice husk gasification, the characteristics of gasification at gasifier temperatures of 700–850 °C were investigated using an ER of 0.20–0.35. As the ER increased, the contents of H₂, CO, and CH₄ decreased and the content of CO₂ increased. The LHV of the product gas and CGE of the gasifier reached a maximum at an ER of 0.20. Therefore, it was confirmed that the optimum ER for gasification was 0.20. On average, the product gas at an ER of 0.20 showed an H₂ content of 2.7%, CO content of 19.2%, CH₄ content of 6.85%, and CO₂

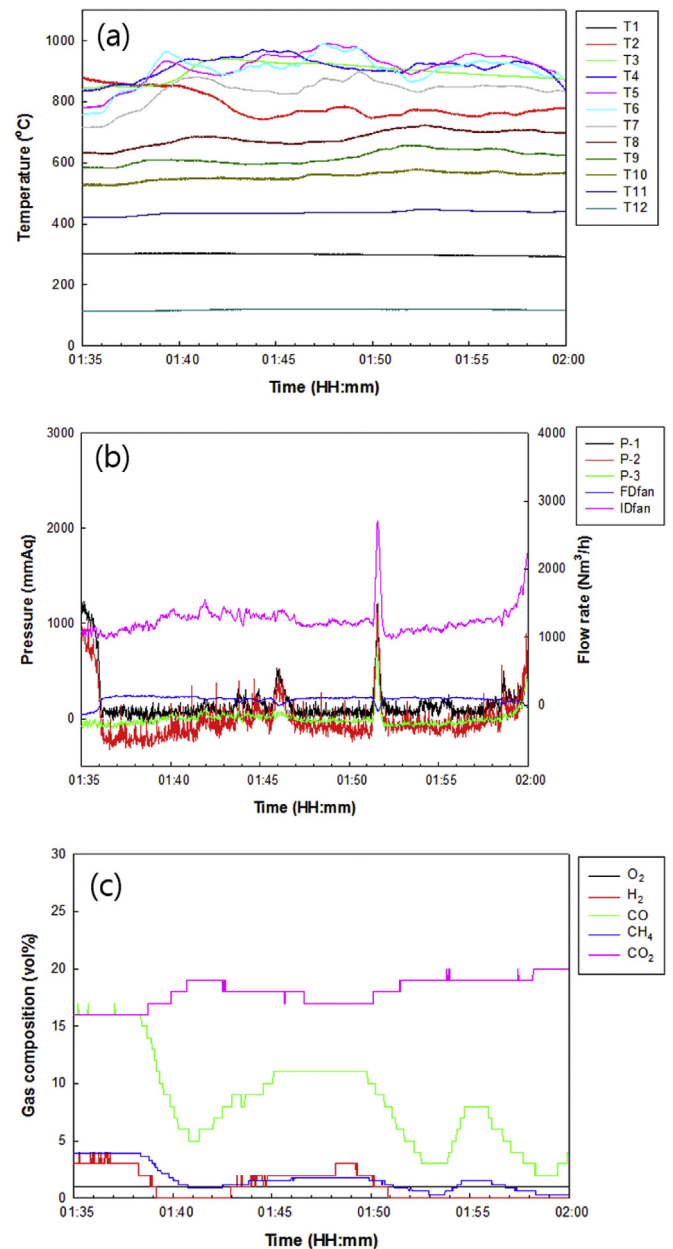


Fig. 4. (a) Temperature, (b) pressure and flow rate, and (c) gas composition during pressure loss.

content of 16.1%. Additionally, the average LHV of the product gas was 1236.6 kcal/Nm³ and the CGE was 61%. The tar content of the product gas both before and after passing through the gas cleaning units was measured and compared. After passing through the gas cleaning unit, the tar content of the product gas was confirmed to be 45.5 mg/Nm³ and the tar removal rate was 98%, which is satisfactory for a gas engine. Pressure loss due to agglomerate formation occurred at the bottom of the gasifier during gasification operations. CPFD simulations were conducted to investigate the fluidizing characteristics caused by agglomerates. To prevent pressure loss caused by agglomerates, it is necessary to remove the agglomerates using an agglomerate removal device; this will maintain the optimum gasification operating conditions for long-term gas engine operations.

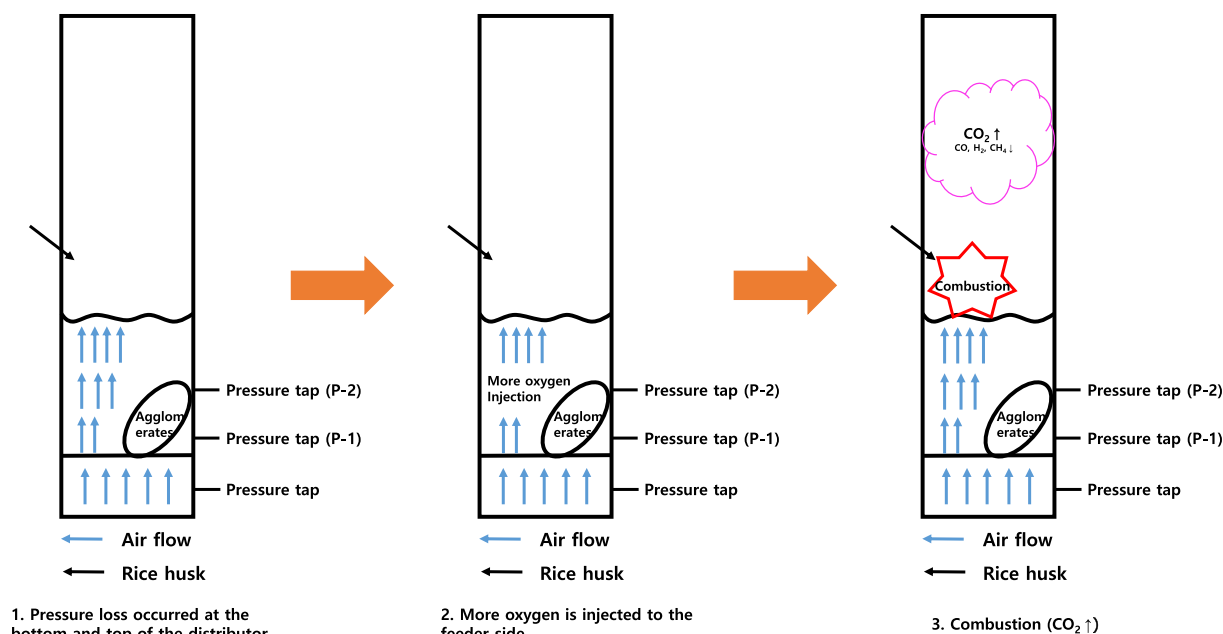


Fig. 5. Schematic diagram of channeling/defluidization phenomenon between the fluidized-bed material and agglomerates.

Table 7
Slagging and fouling index.

Index	Expression/wt%	Slagging/Fouling degree		Rice husk
Base to acid (B/A) ratio	$(\text{Fe}_2\text{O}_3 + \text{CaO} + \text{MgO} + \text{Na}_2\text{O} + \text{K}_2\text{O}) / (\text{SiO}_2 + \text{Al}_2\text{O}_3 + \text{TiO}_2)$	<0.206	Slight	0.09 (Slight)
		0.206–0.4	Moderate	
		>0.4	Severe	
Silica percentage	$\text{SiO}_2 / (\text{SiO}_2 + \text{Fe}_2\text{O}_3 + \text{CaO} + \text{MgO}) \times 100$	72–80	Slight	98.20 (Slight)
		65–72	Moderate	
		50–65	Severe	
Si–Al ratio	$\text{SiO}_2 / \text{Al}_2\text{O}_3$	<1.87	Slight	1291.02 (Severe)
		2.56–1.87	Moderate	
		>2.56	Severe	
B/A alkali	$\text{B/A} \times (\text{Na}_2\text{O} + \text{K}_2\text{O})$	<0.6	Slight	0.56 (Slight)
		0.6–40	Severe	
		>40	Extremely Severe	
B/A sulfide	$(\text{B/A}) \times S_d$, $S_d = \% \text{ of S in dry basis of fuel}$	<0.6	Slight	0.01 (Slight)
		0.6–2.0	Moderate	
		2.0–2.6	Severe	
Chlorine content	Cl amount as received	>2.6	Extremely Severe	0.1 (Sight)
		<0.2	Slight	
		0.2–0.3	Moderate	
Alkali index	Na_2O	0.3–0.5	Severe	0.01 (Slight)
		>0.5	Extremely Severe	
		<2.0	Slight	
	$\text{Na}_2\text{O} + \text{K}_2\text{O}$	>2.0	Severe	6.31 (Severe)
		<3.5	Slight	
		>3.5	Severe	

Table 8
XRF analysis results for the agglomerates from the gasification process.

Sample	SiO ₂	MgO	Fe ₂ O ₃	K ₂ O	Al ₂ O ₃	CaO	Cr ₂ O ₃	MnO	P ₂ O ₅	TiO ₂	Na ₂ O	NiO	BaO	SO ₃	ZnO	Cl	Co ₂ O ₃	V ₂ O ₅	Rb ₂ O
A	70.19	16.71	6.25	2.41	1.72	0.87	0.96	0.43	0.13	0.09	0.07	0.06	0.04	0.03	0.01	0	0.02	0.01	0
B	64.43	22.05	7.7	1.2	2	0.73	1.03	0.41	0.13	0.09	0.06	0.06	0.03	0.02	0.03	0	0.02	0.01	0
C	92.43	0.95	0.48	4.11	0.22	1.18	0.07	0.27	0.13	0	0.07	0.01	0.02	0.02	0	0.03	0	0	0.01

Credit author statement

Sung Jin Park: Conceptualization, Methodology, Writing - Original Draft, Writing - Review & Editing.

Seong Hye Son: Investigation, Data Curation, Visualization.

Jin Woo Kook: Software, Validation.

Ho Won Ra: Investigation, Data Curation, Visualization.

Sang Jun Yoon: Investigation, Data Curation, Visualization.

Tae-Young Mun: Investigation, Data Curation, Visualization.

Ji Hong Moon: Investigation, Data Curation, Visualization.

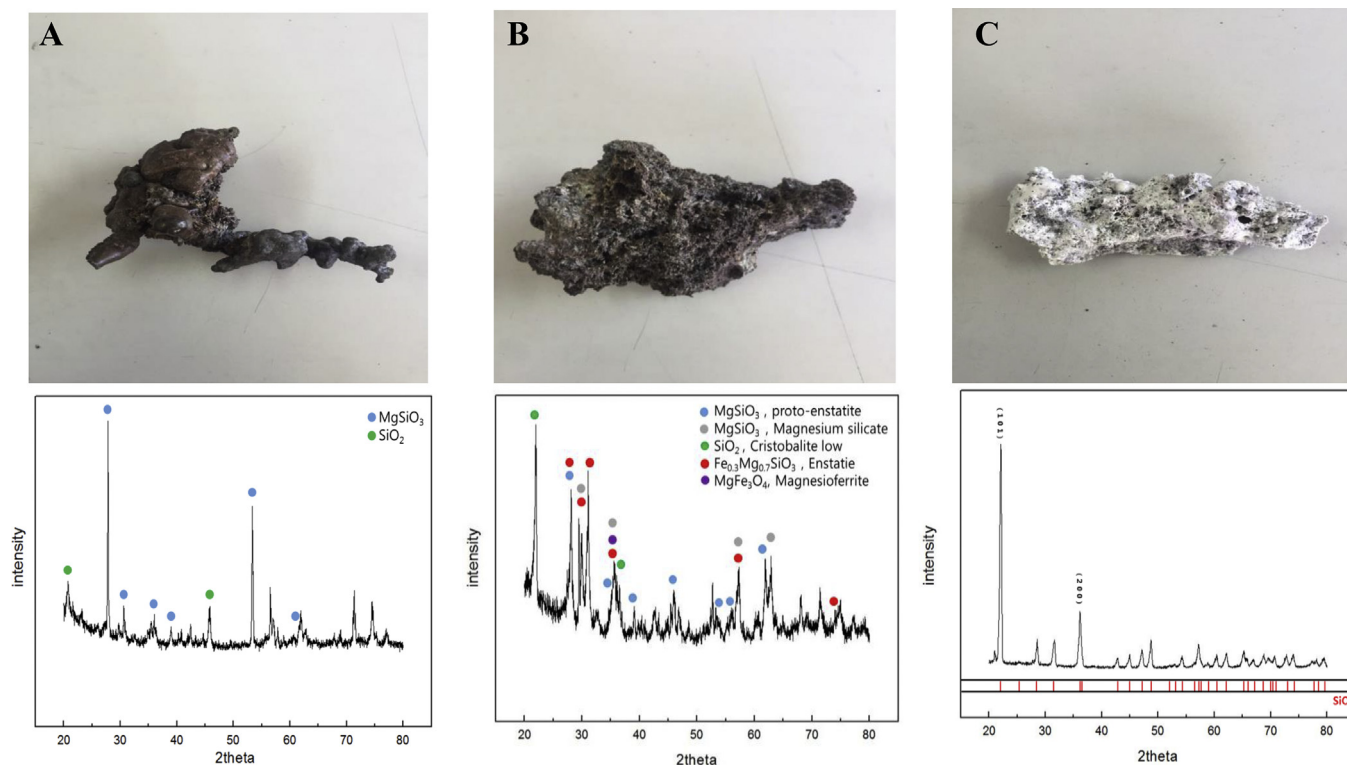


Fig. 6. Picture and XRF spectra of agglomerates from gasifier.

Table 9

Model and parameters used in the simulations.

Drag model		Wen and Yu-Ergun combination [34]
Turbulence model		LES (large-eddy simulation) model [35]
Normal-to-wall momentum retention		0.85
Tangent-to-wall momentum retention		0.85
Maximum momentum redirection from collisions		40%
Restitution coefficient (BGK collision)		No collision model (restitution coefficient: 0.98)
Temperature	Distributor	1073.15 K
	Gasifier	1073.15 K
	Gasifier outlet	1073.15 K
Air velocity ($4U_{mf}$)		0.72 m/s
Gasifier outlet pressure		100772 Pa
Bed material mass		4000 kg
Stacked material		400 kg
Total mass		4400 kg
Amount of total particles		1.79×10^{10}
Amount of total clouds		3.08×10^5
Time step		0.0002 s
Simulation time		60 s

Sung Min Yoon: Formal analysis, Data Curation, Visualization.

Jae Ho Kim: Resources, Investigation.

Yong Ku Kim: Resources, Investigation.

Jae Goo Lee: Supervision, Project administration, Funding acquisition.

Do-Yong Lee: Software, Validation.

Myung Won Seo: Conceptualization, Validation, Writing - Original Draft, Writing - Review & Editing, Supervision.

Declaration of competing interest

The authors declare that they have no known competing financial interests or personal relationships that could have appeared to influence the work reported in this paper.

Acknowledgments

This work was supported by the Korea Institute of Energy Technology Evaluation and Planning (KETEP) and the Ministry of Trade, Industry, & Energy (MOTIE) of the Republic of Korea (No. 20193010093000).

Nomenclature

ER	Equivalence ratio
TPD	Tons per day (ton/day)
CPFD	Computational particle fluid dynamics
CGE	Cold gas efficiency
CDFs	Cooling, demisting, and filter systems

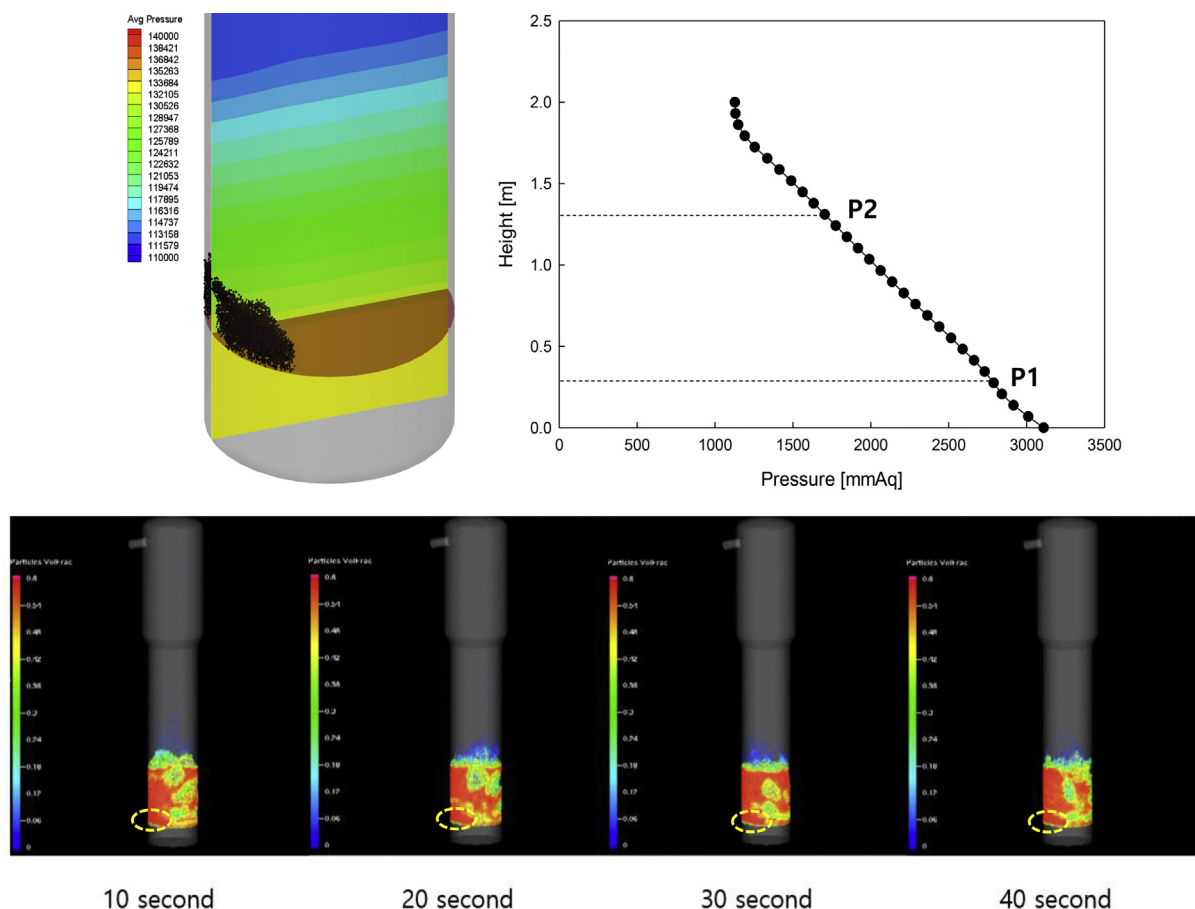


Fig. 7. Average axial pressure profile (top) and solid fraction with simulation time (bottom) from CPFD simulations.

XRF	X-ray fluorescence spectrometry
LHV	Lower heating value
U_{mf}	Minimum fluidizing velocity
FD fan	Forced draft fan
ID fan	Induced draft fan
ND-IR	Non-dispersive infrared gas analyzer
R.T.	Real-time
LES	Large-eddy simulation model

Greek symbols

d	Mean diameter
ρ	Density
Φ	Sphericity
U	Velocity

Subscript

p	Particle
s	Solid
b	Bulk
mf	Minimum fluidization

References

- [1] M. Hiloidhari, D.C. Baruah, Crop residue biomass for decentralized electrical power generation in rural areas (part 1): Investigation of spatial availability, *Renew. Sustain. Energy Rev.* 15 (2011) 1885–1892. <https://doi.org/10.1016/j.rser.2010.12.010>.
- [2] R. Ponde, Potential applications of rice husk ash waste from rice husk biomass power plant, *Renew. Sustain. Energy Rev.* 53 (2016) 1468–1485. <https://doi.org/10.1016/j.rser.2015.09.051>.
- [3] J.W. Kook, H.M. Choi, B.H. Kim, H.W. Ra, S.J. Yoon, T.Y. Mun, J.H. Kim, Y.K. Kim, J.G. Lee, M.W. Seo, Gasification and tar removal characteristics of rice husk in a bubbling fluidized bed reactor, *Fuel* 181 (2016) 942–950. <https://doi.org/10.1016/j.fuel.2016.05.027>.
- [4] W.C. Cho, H.J. Kim, H.I. Lee, M.W. Seo, H.W. Ra, S.J. Yoon, T.Y. Mun, Y.K. Kim, J.H. Kim, B.H. Kim, J.W. Kook, C.Y. Yoo, J.G. Lee, J.W. Choi, 5L-Scale magnesio-milling reduction of nanostructured SiO_2 for high capacity silicon anodes in lithium-ion batteries, *Nano Lett.* 16 (2016) 7261–7269. <https://doi.org/10.1021/acs.nanolett.6b03762>.
- [5] M. Siedlecki, W. de Jong, Biomass gasification as the first hot step in clean syngas production process – gas quality optimization and primary tar reduction measures in a 100 kW thermal input steam-oxygen blown CFB gasifier, *Biomass Bioenergy* 35 (2011) S40–S62. <https://doi.org/10.1016/j.biombioe.2011.05.033>.
- [6] J.F. González, S. Román, D. Bragado, M. Calderón, Investigation on the reactions influencing biomass air and air/steam gasification for hydrogen production, *Fuel Process. Technol.* 89 (2008) 764–772, in: <https://doi.org/10.1016/j.fuproc.2008.01.011>.
- [7] G. Schuster, G. Löffler, K. Weigl, H. Hofbauer, Biomass steam gasification—An extensive parametric modeling study, *Bioresour. Technol.* 77 (2001) 71–79. [https://doi.org/10.1016/S0960-8524\(00\)00115-2](https://doi.org/10.1016/S0960-8524(00)00115-2).
- [8] K. Li, R. Zhang, J. Bi, Experimental study on syngas production by co-gasification of coal and biomass in a fluidized bed, *Int. J. Hydrogen Energy* 35 (2010) 2722–2726. <https://doi.org/10.1016/j.ijhydene.2009.04.046>.
- [9] J.P. Makwana, A.K. Joshi, G. Athawale, D. Singh, P. Mohanty, Air gasification of rice husk in bubbling fluidized bed reactor with bed heating by conventional charcoal, *Bioresour. Technol.* 178 (2015) 45–52. <https://doi.org/10.1016/j.biortech.2014.09.111>.
- [10] M.W. Seo, J.H. Goo, S.D. Kim, S.H. Lee, Y.C. Choi, Gasification characteristics of coal/biomass blend in a dual circulating fluidized bed reactor, *Energy Fuels* 24 (2010) 3108–3118. <https://doi.org/10.1021/ef100204s>.
- [11] T.A. Milne, R.J. Evans, N. Abatzoglou, Biomass Gasifier “Tars”: Their Nature, Formation, and Conversion, National Renewable Energy Laboratory, U.S. Department of Energy, Golden, CO (US), 1998. <https://doi.org/10.2172/3726>.
- [12] P. Subramanian, A. Sampathrajan, P. Venkatachalam, Fluidized bed gasification of select granular biomaterials, *Bioresour. Technol.* 102 (2011) 1914–1920. <https://doi.org/10.1016/j.biortech.2010.08.022>.
- [13] M.K. Karmakar, J. Mandal, S. Haldar, P.K. Chatterjee, Investigation of fuel gas

- generation in a pilot scale fluidized bed autothermal gasifier using rice husk, *Fuel* 111 (2013) 584–591. <https://doi.org/10.1016/j.fuel.2013.03.045>.
- [14] J.J.R. Behainne, J.D. Martinez, Performance analysis of an air-blown pilot fluidized bed gasifier for rice husk, *Energy Sustain. Dev.* 18 (2014) 75–82. <https://doi.org/10.1016/j.esd.2013.11.008>.
 - [15] K.G. Mansaray, A.E. Ghaly, A.M. Al-Taweel, F. Hamdullahpur, V.I. Ugursal, Air gasification of rice husk in a dual distributor type fluidized bed gasifier, *Biomass Bioenergy* 17 (1999) 315–332. [https://doi.org/10.1016/S0961-9534\(99\)00046-X](https://doi.org/10.1016/S0961-9534(99)00046-X).
 - [16] Z.Q. Zhou, L.L. Ma, X.L. Yin, C.Z. Wu, L.C. Huang, C. Wang, Study on biomass circulation and gasification performance in a clapboard-type internal circulating fluidized bed gasifier, *Biotechnol. Adv.* 27 (2009) 612–615. <https://doi.org/10.1016/j.biotechadv.2009.04.016>.
 - [17] J.J. Ramirez, J.D. Martinez, S.L. Petro, Basic design of a fluidized bed gasifier for rice husk on a pilot scale, *Lat. Am. Appl. Res.* 37 (2007) 299–306.
 - [18] X.L. Yin, C.Z. Wu, S.P. Zheng, Y. Chen, Design and operation of a CFB gasification and power generation system for rice husk, *Biomass Bioenergy* 23 (2002) 181–187. [https://doi.org/10.1016/S0961-9534\(02\)00042-9](https://doi.org/10.1016/S0961-9534(02)00042-9).
 - [19] C. Wu, X. Yin, L. Ma, Z. Zhou, H. Chen, Design and operation of a 5.5 MW_e biomass integrated gasification combined cycle demonstration plant, *Energy Fuels* 22 (2008) 4259–4264. <https://doi.org/10.1021/ef8004042>.
 - [20] C.Z. Wu, X.L. Yin, L.L. Ma, Z.Q. Zhou, H.P. Chen, Operational characteristics of a 1.2-MW biomass gasification and power generation plant, *Biotechnol. Adv.* 27 (2009) 588–592. <https://doi.org/10.1016/j.biotechadv.2009.04.020>.
 - [21] C.Y. Wen, Y.H. Yu, A generalized method for predicting the minimum fluidization velocity, *AIChE J.* 12 (1966) 610–612. <https://doi.org/10.1002/aic.690120343>.
 - [22] Mohd Rozainee Taib, Production of Amorphous Silica from Rice Husk in Fluidised Bed System, *Univ Teknol Malaysia*, 2016, p. 362. <https://doi.org/10.1017/CBO9781107415324.004>.
 - [23] D. Geldart, Types of gas fluidization, *Powder Technol.* 7 (1973) 285–292. [https://doi.org/10.1016/0032-5910\(73\)80037-3](https://doi.org/10.1016/0032-5910(73)80037-3).
 - [24] J. Han, Y. Liang, J. Hu, L. Qin, J. Street, Y. Lu, F. Yu, Modeling downdraft biomass gasification process by restricting chemical reaction equilibrium with Aspen Plus, *Energy Convers. Manag.* 153 (2017) 641–648. <https://doi.org/10.1016/j.enconman.2017.10.030>.
 - [25] U. Arena, Fluidized bed gasification, in: F. Scala (Ed.), Chap. 17 in *Fluidized Bed Technologies for Near-Zero Emission Combustion and Gasification*, Woodhead Publishing, 2013, ISBN 978-0-85709-541-1, pp. 765–812. <https://doi.org/10.1533/9780857098801.3.765>.
 - [26] Y. Zhao, S. Sun, H. Tian, J. Qian, F. Su, F. Ling, Characteristics of rice husk gasification in an entrained flow reactor, *Bioresour. Technol.* 100 (2009) 6040–6044. <https://doi.org/10.1016/j.biortech.2009.06.030>.
 - [27] P. Panaka, B.P. Trisaksono, Operating experiences with biomass gasifiers in Indonesia, in: A.V. Bridgwater (Ed.), *Advances in Thermochemical Biomass Conversion*, Springer, 1993, pp. 392–402. https://doi.org/10.1007/978-94-011-1336-6_30.
 - [28] M.W. Seo, G.H. Kim, J.G. Lee, H.M. Jeong, S.M. Jeong, W.J. Lee, S.D. Kim, Carbonization characteristics of biomass/coal blend for bio-coke, in: *The 14th International Conference on Fluidization-From Fundamentals to Products*, 2014.
 - [29] P. Hasler, T.H. Nussbaumer, Gas cleaning for IC engine applications from fixed bed biomass gasification, *Biomass Bioenergy* 16 (1999) 385–395. [https://doi.org/10.1016/S0961-9534\(99\)00018-5](https://doi.org/10.1016/S0961-9534(99)00018-5).
 - [30] P. Pintana, N. Tippayawong, Predicting ash deposit tendency in thermal utilization of biomass, *Eng. J.* 20 (2016) 15–24. <https://doi.org/10.4186/ej.2016.20.5.15>.
 - [31] D.M. Snider, An incompressible three-dimensional multiphase particle-in-cell model for dense particle flows, *J. Comput. Phys.* 170 (2001) 523–549. <https://doi.org/10.1006/jcph.2001.6747>.
 - [32] M.J. Andrews, P.J. O'Rourke, The multiphase particle-in-cell (MP-PIC) method for dense particulate flows, *Int. J. Multiphas. Flow* 22 (1996) 379–402. [https://doi.org/10.1016/0301-9322\(95\)00072-0](https://doi.org/10.1016/0301-9322(95)00072-0).
 - [33] J.H. Lim, K. Bae, J.H. Shin, J.H. Kim, D.H. Lee, J.H. Han, D.H. Lee, Effect of particle-particle interaction on the bed pressure drop and bubble flow by Computational Particle-Fluid Dynamics simulation of bubbling fluidized beds with shroud nozzle, *Powder Technol.* 288 (2016) 315–323. <https://doi.org/10.1016/j.powtec.2015.11.017>.
 - [34] D. Gidaspow, *Multiphase Flow and Fluidization Continuum and Kinetic Theory Description*, Academic Press, Boston, 1994.
 - [35] Y. Shao, J. Gu, Z. Wenqi, A. Yu, Determination of minimum fluidization velocity in fluidized bed at elevated pressures and temperatures using CFD simulations, *Powder Technol.* 350 (2019) 81–90. <https://doi.org/10.1016/j.powtec.2019.03.039>.
 - [36] G. Li, Z. Liu, R. Feng, W. Jiao, Y. Fang, Z. Wang, Conceptual design and analysis of a novel system based on ash agglomerating fluidized bed gasification for co-production of hydrogen and electricity, *Int. J. Hydrogen Energy* 43 (2018) 1980–1988. <https://doi.org/10.1016/j.ijhydene.2017.12.049>.
 - [37] S. Datta, P. Sarkar, P.D. Chavan, S. Saha, G. Sahu, A.K. Sinha, V.K. Saxena, Agglomeration behaviour of high ash Indian coals in fluidized bed gasification pilot plant, *Appl. Therm. Eng.* 86 (2015) 222–228. <https://doi.org/10.1016/j.applthermaleng.2015.04.046>.
 - [38] P. Lahijani, Z.A. Zainal, Gasification of palm empty fruit bunch in a bubbling fluidized bed: a performance and agglomeration study, *Bioresour. Technol.* 102 (2011) 2068–2076. <https://doi.org/10.1016/j.biortech.2010.09.101>.